BIOCHEMISTRY
including biophysical chemistry & molecular biology
Article

Biochemistry **2010,** *49,* 669–678 669
DOI: 10.1021/bi901575h

Photo-Cross-Linking of XPC−Rad23B to Cisplatin-Damaged DNA Reveals Contacts with Both Strands of the DNA Duplex and Spans the DNA Adduct†

Tracy M. Neher,‡ Nadejda I. Rechkunova,§ Olga I. Lavrik,§ and John J. Turchi*,‡,∥

‡*Department of Medicine, Indiana University School of Medicine, Indianapolis, Indiana 46202,* §*Institute of Chemical Biology and Fundamental Medicine, Siberian Branch of the Russian Academy of Sciences, Prospect Lavrentieva 8, Novosibirsk 630090, Russia, and* ∥*Department of Biochemistry and Molecular Biology, Indiana University School of Medicine, Indianapolis, Indiana 46202*

Received September 9, 2009; Revised Manuscript Received November 3, 2009

ABSTRACT: Nucleotide excision repair (NER) is the main pathway used for the repair of bulky DNA adducts such as those caused by UV light exposure and the chemotherapeutic drug cisplatin. The xeroderma pigmentosum group C (XPC)−Rad23B complex is involved in the recognition of these bulky DNA adducts and initiates the global genomic nucleotide excision repair pathway (GG-NER). Photo-cross-linking experiments revealed that the human XPC−Rad23B complex makes direct contact with both the cisplatin-damaged DNA strand and the complementary undamaged strand of a duplex DNA substrate. Coupling photo-cross-linking with denaturation and immunoprecipitation of protein−DNA complexes, we identified the XPC subunit in complex with damaged DNA. While the interaction of the XPC subunit with DNA was direct, studies revealed that although Rad23B was found in complex with DNA, the Rad23B−DNA interaction was largely indirect via its interaction with XPC. Using site specific cross-linking, we determined that the XPC−Rad23B complex is preferentially cross-linked to the damaged DNA when the photoreactive FAP-dCMP (exo-*N*-{2-[*N*-(4-azido-2,5-difluoro-3-chloropyridin-6-yl)-3-aminopropionyl]aminoethyl}-2′-deoxycytidine 5′-monophosphate) analogue is located to the 5′ side of the cisplatin−DNA adduct. When the FAP-dCMP analogue is located to the 3′ side of the adduct, no difference in binding was detected between undamaged and damaged DNA. Collectively, these data suggest a model in which XPC−DNA interactions drive the damage recognition process contacting both the damaged and undamaged DNA strand. Preferential cross-linking 5′ of the cisplatin-damaged site suggests that the XPC−Rad23B complex displays orientation specific binding to eventually impart directionality to the downstream binding and incision events relative to the site of DNA damage.

Lesions, mutations, and bulky adducts caused by internal and external factors such as UV irradiation and environmental carcinogens interfere with DNA replication and transcription and can lead to cell death, cancer, or other diseases (*1*, *2*). Nucleotide excision repair (NER)[1] is a versatile DNA repair pathway utilized for the removal of damaged DNA caused by UV irradiation and platinum-based chemotherapeutic agents used for the treatment of cancer (*1*, *2*). NER is composed of two separate subpathways, transcription-coupled NER (TC-NER) and GG-NER. There are four distinct steps in the NER pathway, including damage recognition, incision of damaged DNA, removal of damage, and resynthesis and ligation of the newly synthesized strand (*1*, *2*). The GG-NER and TC-NER pathways differ only in the method of damage recognition. XPC, Rad23B, and Centrin 2 (CEN2) form the damage recognition complex and are the first proteins to the site of damage in the GG-NER pathway, whereas the stalling of RNA polymerase during transcription is the method of recognition in the TC-NER pathway (*1*, *3*). After recognizing and binding to the damaged DNA, the XPC−Rad23B−CEN2 complex is released, and GG-NER progresses through the excision, repair, and resynthesis steps due to the involvement of more than 30 additional proteins (*2*). RPA and XPA have also been shown to possess damage recognition abilities depending on the type of damage in both GG-NER and TC-NER (*4*). The helicase activity of XPB-TFIIH is responsible for unwinding the damaged DNA followed by 5′ and 3′ incision which is performed by XPF-ERCC1 and XPG, respectively (*5*). Finally, PCNA, RPA, DNA polymerases δ, ε, and κ, and DNA ligases participate in gap filling and ligation of the newly synthesized and repaired DNA (*1*, *2*, *4*, *6*, *7*). More recently, a UV-dependent DNA damage recognition pathway involving DNA-binding protein (DDB) has been shown to recognize and bind to damaged DNA in the absence of XPC (*8*). DDB has been shown to interact with DNA containing UV-induced CPD lesions, which only moderately distort the DNA, suggesting that DDB may play a role in damage recognition of less distorting lesions difficult for XPC to recognize (*9*−*11*).

†This research was supported by Grant R01 CA82741 from the National Institutes of Health (NIH), the National Cancer Institute (J.J.T.), and the Program on Cellular and Molecular Biology RAS (O.I.L.). T.M.N. was supported by the NIH, NRSA T32 CA 111198 Cancer Biology Training Program.

*To whom correspondence should be addressed: Joseph E Walther Hall, R3-C560, Indiana University School of Medicine, 980 W. Walnut St. R3-560, Indianapolis, IN 46202. E-mail: jturchi@iupui.edu. Phone: (318) 278-1996. Fax: (317) 274-0396.

[1]Abbreviations: BSA, bovine serum albumin; CPD, cyclobutane pyrimidine dimer; ds-DNA, double-stranded DNA; DTT, dithiothreitol; EDTA, disodium ethylenediaminetetraacetic acid; EMSA, electrophoretic mobility shift assay; GG-NER, global genomic nucleotide excision repair; IP, immunoprecipitation; NER, nucleotide excision repair; Pt, cisplatin; RPA, replication protein A; TFIIH, transcription factor II H; XPA, -C, -F, and -G, xeroderma pigmentosum group A, C, F, and G proteins, respectively.

Published on Web 12/22/2009

In vivo, human XPC (125 kDa) forms a heterotrimeric complex with the 58 kDa protein Rad23B along with the 18 kDa protein Centrin 2 (*12*). In vitro, XPC and Rad23B are sufficient for reconstituting the damage recognition complex responsible for the initiation of NER (*13*, *14*), and the XPC−Rad23B complex preferentially binds to cisplatin and UV-damaged double-stranded DNA in the presence of the non-specific competitor poly-dI/dC (*4*, *15*−*18*). In addition, the XPC−Rad23B complex (XPC−Rad23B) recognizes a variety of chemically and structurally diverse DNA adducts, and previously published data have shown that the more distorting the damage the higher affinity XPC−Rad23B demonstrates for the damaged DNA (*19*). It has been suggested that XPC−Rad23B interacts with the undamaged strand of a damaged duplex DNA via the single strand characteristics caused by the bulky UV or cisplatin lesions (*16*, *20*). These data are supported by the structural analysis of yeast Rad4, the XPC orthologue, and Rad23B bound to DNA containing a cyclobutane pyrimidine dimer (CPD) lesion where Rad4 contacts were identified on both the undamaged strand of the duplex and base pairs surrounding the CPD lesion (*21*) . The transglutaminase homology domain (TGD) and long β-hairpin domain 1 (BHD1) bind to the undamaged strand to the 3′ side of the CPD lesion. β-Hairpin domains 2 and 3 (BHD2 and BHD3, respectively) bind to the DNA containing the CPD lesion and cause the two base pairs opposite of the lesion to flip outward (*21*). In a comparison of the DNA-absent (apo) model to the DNA-bound model, BHD2 and BHD3 move approximately 8−12 Å relative to the position of the DNA. This flexibility is thought to aid in damage recognition and binding of Rad4 and possible XPC to damaged duplex DNA. As the sequence of Rad4 is 23% identical with that of XPC, it is unclear, however, if XPC will bind to DNA in the same manner as Rad4. It is also unclear whether other lesions, which result in different structural distortions but are still repaired by NER, will be recognized using the same series of interactions. To address this latter question, we examined the interaction of XPC−Rad23B with cisplatin-damaged DNA focusing on specific protein−DNA interactions.

Cisplatin is a common chemotherapeutic agent used for the treatment of several cancers, including testicular, lung, and ovarian cancer (*22*−*25*). 1,2-d(GpG) cisplatin adducts are the most common lesions and distort the DNA ∼13°, while 1,3-d(GpXpG) causes an ∼27−33° kink in the DNA around the platinum lesion and makes up a much smaller portion of the cisplatin intrastrand lesions (*26*, *27*). Although XPC−Rad23B recognizes the bulky adduct, it remains unclear if XPC−Rad23B contacts the cisplatin lesion directly. It is also unknown if XPC−Rad23B demonstrates preferential binding either 5′ or 3′ to the site of cisplatin damage or if the protein symmetrically spans the lesion. Determining the general location of XPC−Rad23B in relation to the cisplatin adduct will give directionality to XPC−Rad23B and possibly downstream NER proteins. Protein directionality will provide insight into the mechanism of XPC−Rad23B damage recognition which is versatile and unclear. It may also aid in the determination of the placement of downstream NER proteins, such as XPF and XPG which are important for excision of the damaged bases and the excision product removed. To further probe the nature of the XPC−Rad23B−DNA interactions, we undertook a photo-cross-linking approach using a series of cisplatin-damaged DNA substrates. To further increase the efficiency, specificity, and resolution of the approach, a photoreactive exo-*N*-{2-[*N*-(4-azido-2,5-difluoro-3-chloropyridin-6-yl)-3-aminopropionyl]aminoethyl}-2′-deoxycytidine 5′-triphosphase (FAP-dCTP) analogue was used to introduce photoreactive residues into specific positions of the DNA substrate. FAP-dCTP is a dCTP analogue that contains a photoreactive FAP group inserted at the 4-C location and aids in the cross-linking efficiency of substrates (*28*). Results demonstrate strand and orientation specific binding of the XPC subunit in complex with Rad23B to DNA containing the cisplatin adduct. These results provide an improved understanding of the XPC−DNA interaction and provide details that may allow improvement of platinum-based chemotherapeutic treatments possibly through direct inhibition of XPC or development of a platinum-based therapeutic which XPC cannot recognize.

EXPERIMENTAL PROCEDURES

Chemicals. Cisplatin was purchased from Sigma-Aldrich (St. Louis, MO), and [γ-^{32}P]ATP was supplied by Perkin-Elmer (Waltham, MA). Oligonucleotides were purchased from Integrated DNA Technologies (Coralville, IA). Klenow Fragment 3′−5′ exo$^-$, T4 polynucleotide kinase (T4 PNK), T4 DNA ligase, and HaeIII were purchased from New England Biolabs (Ipswich, MA). Phosphocellulose (Whatman P-11) was obtained from Fisher Scientific (Houston, TX) along with T4 DNA polymerase. ssDNA cellulose was obtained from Sigma Chemical Co. (St. Louis, MO). Protein-G agarose, XPC, and Rad23B rabbit polyclonal antibodies were purchased from Santa Cruz Biotechnology (Santa Cruz, CA). Streptavidin MagneSphere Paramagnetic Particles were purchased from Promega (Madison, WI). The photoreactive analogue of dCTP, exo-*N*-{2-[*N*-(4-azido-2,5-difluoro-3-chloropyridin-6-yl)-3-aminopropionyl]aminoethyl}-2′-deoxycytidine 5′-triphosphate (FAP-dCTP), was synthesized as described previously (*28*).

Protein Purification. XPC and Rad23B were purified from SF-9 insect cells to near homogeneity as previously described (*16*). Briefly, SF-9 cells (500 mL) were infected (10 plaque forming units/cell) with recombinant baculovirus expressing XPC−Rad23B passage-2 virus and incubated at 27 °C. After 48 h, a cell-free extract was prepared as described by Manley et al. (*29*). Briefly, cells were lysed in a hypotonic buffer [10 mM Tris-HCl (pH 8.0), 1 mM EDTA, and 5 mM DTT] followed by a high-salt buffer [50 mM Tris-HCl (pH 8.0), 10 mM $MgCl_2$, 2 mM DTT, 25% (w/v) sucrose, and 50% (v/v) glycerol]. The sample was centrifuged at 30000*g* for 1 h, and the supernatant was dialyzed overnight in buffer A [25 mM Tris-HCl (pH 7.5), 1 mM EDTA, 1 mM DTT, 0.001% (v/v) Triton X-100, and 10% (v/v) glycerol] containing 0.3 M NaCl. Following centrifugation, the clarified supernatant was applied to a 10 mL P-cell column equilibrated in buffer A containing 0.3 M NaCl. The column was washed with 0.3 M NaCl with buffer A, and protein was eluted from the column using 1 M NaCl with buffer A. XPC−Rad23B-containing fractions were pooled and diluted with buffer A to achieve a final salt concentration of 0.6 M. The diluted protein pool was applied to a 4 mL ssDNA column equilibrated in 0.6 M NaCl with buffer A. The column was washed, and protein was eluted from the column using 1.5 M NaCl with buffer A. XPC−Rad23B-containing fractions were pooled and dialyzed overnight in buffer B [25 mM HEPES (pH 7.8), 0.2 M KCl, 1 mM EDTA, 1 mM DTT, and 50% (v/v) glycerol]. Final protein concentrations were determined using a Bradford dye-based assay (Bio-Rad), and the dialyzed protein was aliquoted and stored at −80 °C. SDS−PAGE followed by Coomassie staining or Western blot analysis was utilized to determine protein purity.

Table 1: DNA Oligonucleotides

DNA	sequence (5′−3′)
1,2-d(GpG)[a]	CCCTTCTTTCTCTTCCCCCTCTCCTTCTTGGCCTCTTCCTTCCCCTTCCCTTTCCTCCCC
C-1,2-d(GpG)	GGGGAGGAAAGGGAAGGGGAAGGAAGAGGCCAAGAAGGAGAGGGGGAAGAGAAAGAAGGG
5′FAP1[b]	CCCTTCTTTCTCTTCCCCCTAT*C*
5′FAP2[a]	TCTCTTGGCCTCTCTCTTCCCCTTCCCTTTCCTCCCC
3′FAP1[a,b]	CCCTTCTTTCTCTTCCCCCTATCTCTCTTGGCCTCTCT*C*
C-FAP	AGGGGAGGAAAGGGAAGGGGAAGAGAGAGGCCAAGAGAGATAGGGGGAAGAGAAAGAAGGG

[a]Underlined bases indicate the site for cisplatin damage. [b]The italic base indicates the incorporated photoreactive FAP-dCTP analogue.

XPC−Rad23B DNA binding activity was assessed using fluorescence polarization on a fluorescein-labeled DNA substrate (56-mer) in a 500 μL reaction volume containing 20 mM HEPES (pH 7.8), 1 mM DTT, 0.01% (v/v) NP-40, and 100 mM NaCl (*16*). XPC−Rad23B was titrated to a final concentration of 200 μM. Activity was also assessed using an electrophoretic mobility shift assay (EMSA) on undamaged or cisplatin-damaged substrates (60-mer) (*16*).

DNA Substrates. All oligonucleotides (22-, 37-, 38-, 60-, and 61-mers) (Table 1) were purified by electrophoresis on denaturing polyacrylamide gels and precipitated with ethanol, and the concentration was determined using a Nanodrop 1000 instrument (Nanodrop Technologies). Damage was induced by incubating the purified oligonucleotides with cisplatin at a drug: molecule ratio of 10:1 in buffer containing 1 mM $NaHPO_4$ (pH 7.5) and 3 mM NaCl for 48 h. Damaged DNA was quantified using the Nanodrop 1000 instrument (Nanodrop Technologies) following ethanol precipitation (*16*).

Radiolabeled (5′) DNA was prepared by incubation of undamaged or cisplatin-damaged oligonucleotides with [γ-^{32}P]-ATP, T4 PNK, and kinase buffer at 37 °C. After incubation for 30 min, 1 mM ATP was added followed by 0.5 M EDTA, and then the DNA was purified using a G50 spin column. The counts per minute (CPM) were measured using a scintillation counter (Beckman), and the specific activity and DNA concentrations were calculated. Undamaged and damaged substrates were annealed to the complement strand, C-1,2-d(GpG), by being heated to 95 °C for 3 min in annealing buffer [50 mM Tris (pH 7.5), 10 mM magnesium acetate, and 5 mM DTT] to generate ds-(GpG). Double-stranded cisplatin-damaged substrates were subjected to HaeIII digestion, and 60-mer products were purified by electrophoresis on native polyacrylamide gels. The site of platination resides within the HaeIII digestion site; therefore, any substrate not platinated is cleaved by HaeIII to a 30-mer, whereas platinated substrates remain 60-mers.

Oligonucleotides possessing the photoreactive analogue of dCMP, exo-*N*-{2-[*N*-(4-azido-2,5-difluoro-3-chloropyridin-6-yl)-3-aminopropionyl]aminoethyl}-2′-deoxycytidine 5′-monophosphase (FAP-dCMP), were prepared by extension reactions catalyzed by Klenow polymerase 3′−5′ exo$^-$ and ligation catalyzed by T4 DNA ligase. Duplex DNA substrates were prepared with the FAP-dCMP either 5′ (ds-5′FAP) or 3′ (ds-3′FAP) of the cisplatin adduct (Figure 1 of the Supporting Information). 5′FAP1 and 3′FAP1 were 5′ radiolabeled, and control (undamaged) and cisplatin-damaged 5′FAP2 was cold-phosphorylated and excess ATP removed by Sephadex G50 spin column chromatogrphy. Radiolabeled control or damaged 5′FAP1 and 5′FAP2 were annealed to the complementary strand (C-FAP), and fill-in reactions performed with FAP-dCTP followed by ligation were used to generate control and cisplatin-damaged ds-5′FAP. Radiolabeled control or cisplatin-damaged 3′FAP1 was annealed to C-FAP, extended with the FAP-dCTP analogue, and purified via Sephadex G50 spin column chromatography. The substrates were incubated with dCTP, dTTP, and Klenow polymerase 3′−5′ exo$^-$ for an additional 30 min at 37 °C to complete synthesis of the substrate generating control or cisplatin-damaged ds-3′FAP. The free dNTPs were removed using Sephadex G50 spin column chromatography, and cisplatin-damaged substrates were digested with HaeIII (see above), purified by electrophoresis on a preparative denaturing polyacrylamide gel, and re-annealed.

Electrophoretic Mobility Shift Assay (*EMSA*). XPC−Rad23B was bound to 100 fmol of undamaged or cisplatin-damaged ds-DNA (60-mer) in buffer containing 20 mM HEPES (pH 7.8), 0.001% (v/v) NP-40, 50 mM NaCl, 1 mM DTT, 0.05 mg/mL BSA, and 2 mM $MgCl_2$. Binding was performed for 15 min at room temperature in the absence or presence of nonspecific competitor poly-dI/dC (100 ng). Bound XPC−Rad23B was cross-linked via glutaraldehyde to the substrates, by the addition of 0.25% (v/v) glutaraldehyde and incubation of the samples at room temperature for 3 min. Buffer containing 10 mM EDTA, 10% glycerol, 0.01% bromophenol blue, and 0.01% xylene cyanol was used to stop the reactions, and samples were separated on native polyacrylamide gels for 1 h at 170 V. Dried gels were imaged using a Storm 820 PhosphorImager (Amersham Biosciences), and bound protein was quantified using ImageQuant version 5.2. Averages and standard deviations of three independent experiments are presented.

Photo-Cross-Linking and SDS−PAGE Analysis. Binding to cisplatin-damaged or undamaged/control DNA substrates was performed in the presence or absence of poly-dI/dC, as stated above. Samples were then photo-cross-linked in Eppendorf tubes, on ice, by UV irradiation using General Electric 15 W bulbs that emit a wavelength of 254 nm, for the indicated times. Following cross-linking, 6× SDS dye was used to stop the reactions and samples were heated to 95 °C for 5 min and loaded on SDS−PAGE gels. Gels were imaged and quantified using a Storm 820 PhosphorImager (Amersham Biosciences) and ImageQuant version 5.2. Averages and standard deviations from at least three independent experiments are presented.

Immunoprecipitation (*IP*). XPC−Rad23B was bound to the indicated undamaged/control or cisplatin-damaged ds-DNA (600 fmol) and photo-cross-linked for the indicated times. Photo-cross-linked samples were incubated for 20 min with either XPC or Rad23B rabbit polyclonal antibodies with and without a denaturation step (10 min at 95 °C) prior to incubation with the antibody. Protein-G agarose was washed three times with PBS and added to each sample along with PBS buffer, and the samples were rotated at 4 °C for 1.5 h. Samples processed after IP were washed three times with PBS, resuspended in 1× SDS dye, and

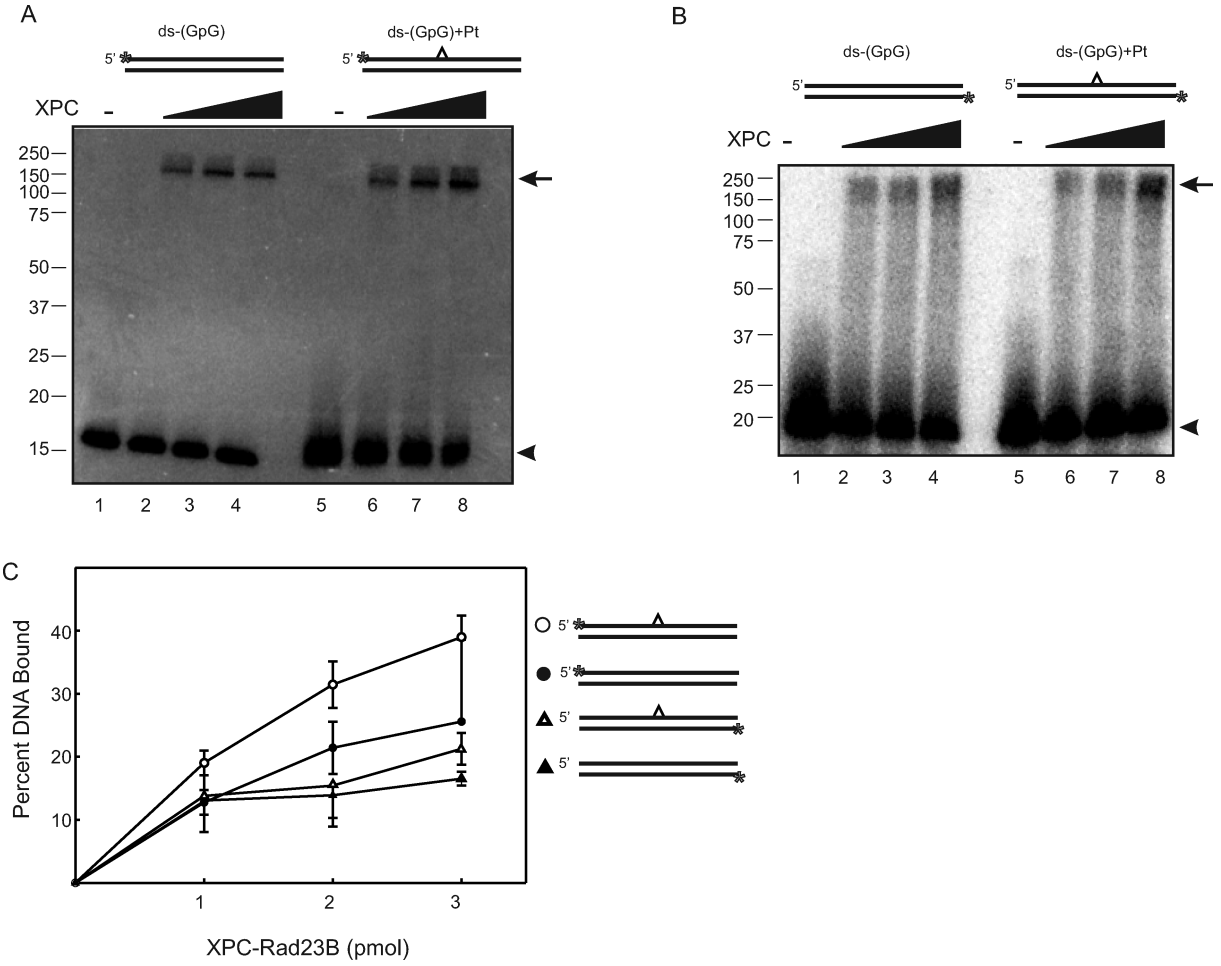

FIGURE 1: XPC−Rad23B photo-cross-links to undamaged and cisplatin-damaged DNA. (A) Increasing amounts of XPC−Rad23B were incubated with undamaged or cisplatin-damaged ds-DNA with the ^{32}P label on the damaged strand and photo-cross-linked for 60 min. Samples were heat denatured and separated via SDS−PAGE, and radioactivity was detected by PhosporImager analysis. (B) Similar cross-linking reactions were performed except the ^{32}P label was positioned on the DNA strand complementary to the damaged DNA strand. A schematic of each DNA substrate is depicted above the gels with the cisplatin indicated by the carat and the position of the ^{32}P label by the asterisk. The covalent protein−DNA complex is indicated by the arrow and the free DNA by the arrowhead. (C) Quantification of XPC−Rad23B photo-cross-linked to double-stranded undamaged or cisplatin-damaged substrates presented in panels A and B.

loaded onto SDS−PAGE gels. Western blot analysis using either a primary XPC or Rad23B antibody (1:1000) and a goat anti-rabbit secondary antibody (1:2000) was used along with chemiluminescense to visualize the results. A Fuji LAS-3000 camera along with Multi Gauge verison 3.0 was used to visualize the results. Radiolabeled substrates were also separated using SDS−PAGE, and dried gels were imaged using a Storm 820 PhosphorImager (Amersham Biosciences).

RESULTS

XPC−Rad23B Covalently Photo-Cross-Links to Undamaged and Cisplatin-Damaged DNA. We and others have analyzed the interaction of XPC−Rad23B with DNA by a variety of biochemical techniques and assays (*15*, *16*, *19*, *30*). XPC−Rad23B demonstrates damage specificity only in the presence of the nonspecific competitor poly-dI/dC, a synthetic double-stranded oligonucleotide. XPC−Rad23B often requires glutaraldehyde cross-linking for the identification of the presence of protein−DNA complexes (*16*). To further analyze the specifics of interactions of XPC−Rad23B with DNA, we employed DNA containing a single cisplatin lesion in conjunction with site specific photoreactive dCMP residues. XPC−Rad23B was purified to near homogeneity from insect cells using a recombinant baculovirus construct. Preliminary experiments involved fluorescence polarization, and an EMSA with glutaraldehyde cross-linking confirmed the DNA binding activity of XPC−Rad23B. XPC−Rad23B was shown to bind to a fluorescein-labeled substrate (56-mer), and glutaraldehyde cross-linking demonstrated damaged specificity in the presence of competitor poly-dI/dC, confirming previously published results (*16*).

Photo-cross-linking of XPC−Rad23B to radiolabeled DNA was conducted by first binding XPC−Rad23B to ds-(GpG) with or without a site specific 1,2-d(GpG) cisplatin lesion (Table 1). XPC−Rad23B was photo-cross-linked to these DNA derivatives for 1 h, and SDS−PAGE gels were utilized to separate the covalent protein−DNA complexes. Preliminary experiments involving UV exposure time course analysis revealed 1 h to be optimal for protein stability and cross-linking efficiency (data not shown). PhosphorImager analysis reveals the presence of two bands in reaction mixtures containing radiolabeled DNA duplexes and XPC−Rad23B. The lower band migrating at approximately 15 kDa corresponds to unbound DNA, and the upper band (170 kDa) corresponds to a covalent protein−DNA complex (Figure 1A). The amount of this covalent protein−DNA complex increased with increasing concentrations of XPC−Rad23B, whereas the the amount of unbound DNA

decreases. In the data presented and quantification of triplicate binding experiments, XPC−Rad23B revealed preferential cross-linking to cisplatin-damaged DNA (Figure 1C). However, the results were variable, and in some preparations of XPC−Rad23B, there was a smaller difference in photo-cross-linking of the protein to undamaged and cisplatin-damaged DNA. Similar experiments involving photo-cross-linking of XPC−Rad23B to a damaged ds-DNA substrate (60-mer) containing a site specific 1,3-d(GpXpG) cisplatin lesion also reveal damage specific cross-linking (Figure 2 of the Supporting Information). As stated above, XPC−Rad23B glutaraldehyde cross-links more efficiently to undamaged DNA in the absence of a competitor (data not shown). Therefore, the observed increase in the level of photo-cross-linking of XPC−Rad23B to cisplatin-damaged DNA suggests there is either a platinum damage-dependent alteration in XPC structure that is more efficiently cross-linked to the DNA bases or, more likely, a direct platinum−protein cross-link. The precedence for UV-dependent direct platinum−protein cross-links has been established in the analysis of binding of HMGB-1 to a single cisplatin-damaged DNA (*31*). This interpretation would position XPC in the direct proximity of the DNA adduct, consistent with the recently reported Rad4 crystal structure in conjunction with a CPD lesion (*21*).

XPC−Rad23B Covalently Photo-Cross-Links to the Undamaged Complementary Strand. Data presented above demonstrate that XPC−Rad23B is able to bind and photo-cross-link to cisplatin-damaged and undamaged DNA, demonstrating a preference for damaged DNA. However, it is not known if, in the context of a duplex DNA containing a single cisplatin lesion, XPC−Rad23B can make contact with the undamaged complementary DNA strand. To visualize whether XPC−Rad23B binds to the undamaged complement strand, DNA substrates were prepared with a 5′ ^{32}P label located on the undamaged strand. After binding and photo-cross-linking, SDS−PAGE gels were used to separate the cross-linked products and a PhosphorImager was utilized to visualize the results. Again, only covalent interactions will remain intact when separated on SDS−PAGE gels. Therefore, if XPC−Rad23B is not covalently bound to the undamaged complement strand, only free DNA would be expected (15 kDa). However, data reveal the presence of a high-molecular mass band (170 kDa) representative of a protein−DNA photoinduced covalent cross-link (Figure 1B). Quantification of the data (Figure 1C) indicates the amount of the cross-linked product observed when the undamaged strand is labeled with ^{32}P is smaller than that observed in reactions with the damaged strand labeled with ^{32}P. These results suggest that XPC and possibly Rad23B not only make contact with the damaged strand of duplex DNA but also interact with the complementary undamaged strand of the damaged DNA duplex (Figure 1). Therefore, XPC forms direct contacts with both strands of an undamaged DNA duplex (Figure 1A,B). While the photo-cross-linking reactions were internally controlled, irradiation with UV light for 60 min can impact numerous factors, including UV-induced DNA damage and decreases in overall protein stability. Control experiments were conducted in which the DNA was UV irradiated and then used in an XPC−Rad23B binding reaction with glutaraldehyde cross-linking. The results demonstrate no significant increase in the level of protein−DNA complex formation versus the control experiment in which the DNA was not UV irradiated prior to glutaraldehyde cross-linking (data not shown). In addition, SDS−PAGE analysis of the protein following UV irradiation revealed no significant degradation of the XPC or Rad23B subunits (data not shown). Despite the controls which indicated that there was not extensive UV-induced damage to the substrate, the cross-linking efficiency is still relatively poor; thus, we sought a more efficient methodology with increased resolution to characterize the protein−DNA complexes formed on cisplatin-damaged DNA.

XPC−Rad23B Covalently Photo-Cross-Links to Photoreactive Substrates. Previously, halogenated bases have been used to improve cross-linking efficiency in experiments involving photoaffinity labeling of proteins. However, only small increases in photo-cross-linking efficiency have been shown (*32*). More recently, photoactivateable cross-linkers have been synthesized as dNTP analogues which allow for their site specific placement into DNA as a photoreactive dNMP moiety which results in significantly increased cross-linking efficiency (*28*, *33*, *34*). Oligonucleotides possessing a photoreactive FAP-dCMP analogue, to the 5′ or 3′ side of the cisplatin damage site, were prepared as described in Experimental Procedures. Photo-cross-linking experiments were again conducted with DNA substrates that contained FAP-dCMP moieties and were exposed to UV light for only 10 min versus the 60 min exposure for dCMP-containing substrates. The significant decrease in UV exposure reduces the likelihood of UV-induced damage to the DNA substrates and protein which may influence binding and cross-linking. SDS−PAGE and PhosphorImager analysis were utilized for sample separation and visualization of the cross-linking results. Data reveal that XPC−Rad23B photo-cross-links significantly more efficiently to substrates possessing FAP-dCMP than an identical substrate possessing dCMP. The data presented in Figure 2A demonstrate that photo-cross-linking for 60 min with the control substrate (dCMP) still resulted in less covalent protein−DNA complex being detected compared to a 10 min exposure with the FAP-dCMP-containing substrate. The FAP-dCMP substrate cross-links with itself in the absence of XPC−Rad23B; however, this interaction is eliminated in the presence of XPC−Rad23B and does not inhibit a protein−DNA interaction (Figure 2A). In a comparison of control and cisplatin-damaged substrates containing FAP-dCMP, XPC does not demonstrate damage specific binding when the photoreactive substrate is to the 5′ or 3′ side of the analogue (Figure 2B,C and Figure 3A,B of the Supporting Information). This result suggests that the FAP-dCTP analogue causes some degree of distortion with which XPC−Rad23B can recognize and interact. Data demonstrate that XPC−Rad23B cross-links slightly more efficiently to substrates containing a 5′-located photoreactive analogue versus a 3′ photoreactive analogue (Figure 3). A comparison of the data presented in Figure 3B is significant to a P value of < 0.05. These data demonstrate that XPC−Rad23B has a preference for interacting to the 5′ side of the site of damage. However, the ability to detect protein−DNA interactions to the 3′ side of the cisplatin lesion suggests the protein spans the damage to enable contacts on both sides of the cisplatin lesion. Overall, these data provide an improved understanding of where XPC−Rad23B contacts the damaged DNA; more specifically, XPC−Rad23B contacts the DNA both 5′ and 3′ of the cisplatin lesion, demonstrating a preference for contacting the 5′ side of the lesion.

XPC−Rad23B Subunits Covalently Photo-Cross-Link in the Absence and Presence of DNA. The mobility of the covalent protein−DNA complex (170 kDa) presents the possibility that either XPC alone or XPC in complex with Rad23B is

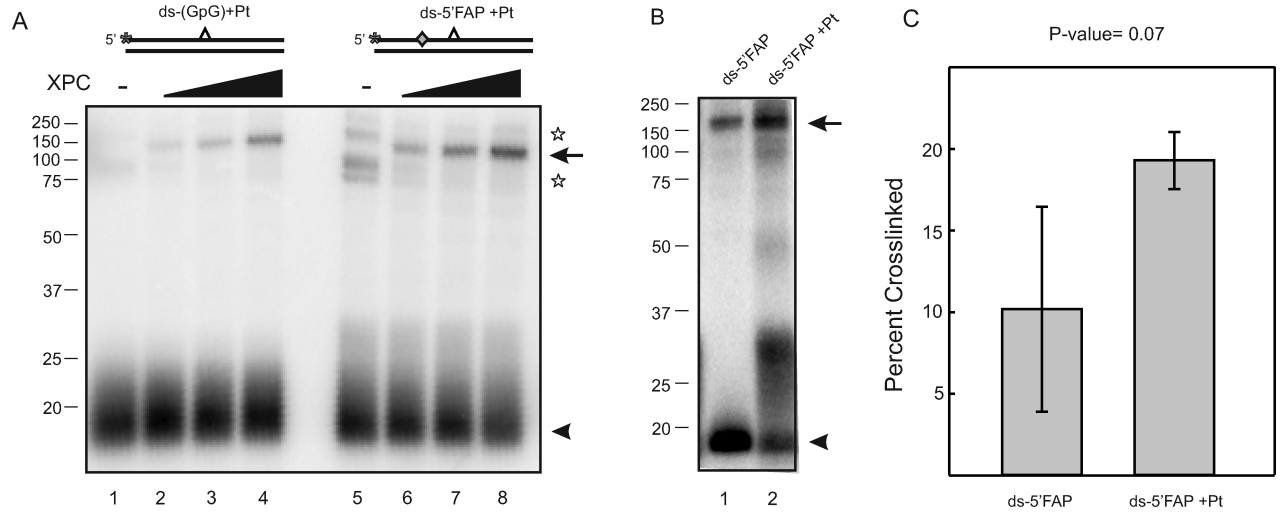

FIGURE 2: Damage specificity of XPC−Rad23B photo-cross-links revealed by a photoreactive FAP-dCTP analogue. (A) Increasing amounts of XPC−Rad23B (2, 4, and 6 pmol) were incubated with cisplatin-damaged control or FAP-dCMP-modified ds-DNA with the ^{32}P label on the damaged strand and photo-cross-linked for 60 min (lanes 1−4) or 10 min (lanes 5−8). Samples were heat denatured and separated via SDS−PAGE, and radioactivity was detected by PhosporImager analysis. The stars indicate a photoinduced DNA cross-link observed in the absence of XPC−Rad23B. (B) Similar cross-linking reactions were performed with the FAP-dCMP modified using either control (lane 1) or cisplatin-damaged DNA (lane 2). The covalent protein−DNA complex is indicated by the arrow and the free DNA by the arrowhead. A schematic of each DNA substrate is depicted above the gels with the cisplatin indicated by the carat, the position of the ^{32}P label by the asterisk, and the position of the FAP-dCMP by the diamond. (C) Quantification of three independent cross-linking experiments to compare the efficiency of cross-linking of XPC−Rad23B to a cisplatin-damaged or control substrate. A P value of 0.07 was determined by a paired Student's t test.

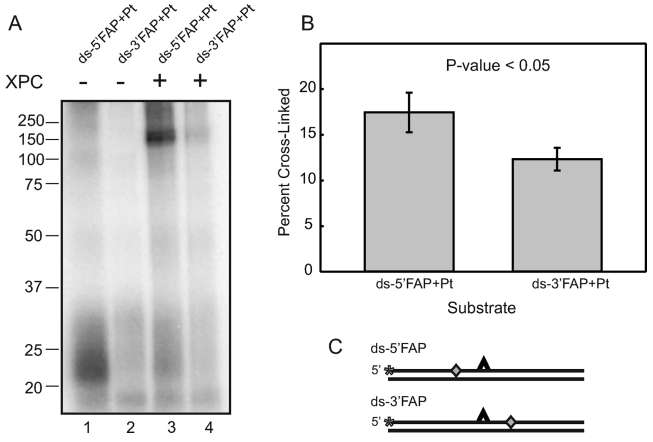

FIGURE 3: Orientation of XPC−Rad23B bound to cisplatin-damaged DNA. (A) XPC−Rad23B (6 pmol) was incubated and photo-cross-linked for 10 min to cisplatin-damaged substrates containing a 5′ (lanes 1 and 3) or 3′ (lanes 2 and 4) photoreactive FAB-dCMP analogue. Products were separated by SDS−PAGE and visualized by PhosphorImager analysis. (B) Quantification of the binding data from three independent cross-linking experiments. A paired t test was utilized to determine the statistical significance (P value of < 0.05). (C) Schematic of DNA substrates with the cisplatin indicated by the carat, the position of the ^{32}P label by the asterisk, and the position of the FAP-dCMP by the diamond.

present in the cross-linked product. The absence of a product with a mobility ranging between 60 and 100 kDa suggests that Rad23B alone is not in complex with the DNA. To determine if Rad23B is present in the 170 kDa covalent protein−DNA complex, we extended the cross-linking analysis to include IP after a heat denaturation step used to disrupt the noncovalent protein−protein and protein−DNA complexes. In doing so, we found only remaining covalent interactions would be pulled down with IP and detected via SDS−PAGE. Results demonstrate that both the XPC and Rad23B antibody are capable of pulling down a photoinduced covalent protein−DNA complex (Figure 4A). A similar analysis, in which the undamaged complementary strand of the duplex was radiolabeled, revealed significantly less cross-linking which is apparent in that overexposure is necessary to detect the complexes (Figure 4B). In addition, quantification of the signal intensity revealed a higher level of binding to the undamaged DNA compared to the cisplatin-damaged DNA (24% bound vs 7%).

The ability to pull down a protein−DNA complex with anti-Rad23B suggests that Rad23B is in direct contact with DNA or was covalently photo-cross-linked to XPC. To further study the nature of these interactions, we probed for each component using Western blot analysis. In these experiments, samples were UV irradiated for the indicated times and immunoprecipitated with either anti-XPC (data not shown) or anti-Rad23B without a heat denaturation step (Figure 5A) or following heat denaturation (Figure 5B). The control experiments performed without prior heat denaturation demonstrate, as expected, that anti-Rad23B could pull down XPC in the presence or absence of DNA (Figure 5A, lanes 1, 3, and 4). Exposure to UV light reveals a decrease in the intensity of the XPC protein migrating at 125 kDa and the appearance of a smear of products with significantly reduced mobility consistent with covalently interacting XPC−Rad23B complexes (Figure 5A, lanes 2, 5, and 6). Interestingly, when samples were photo-cross-linked and heat denatured prior to being pulled down with the anti-Rad23B antibody, an XPC−Rad23B complex with reduced mobility was still detected (Figure 5B, lanes 2, 5, and 6). These results are consistent with the generation of a photoinduced covalent bond between the XPC and Rad23B subunits in the absence or presence of DNA. Data revealed that the presence of DNA had a minimal effect on the photoinduced XPC−Rad23B covalent complexes (in Figure 5A,B, compare lane 3 to lane 5 and lane 4 to lane 6). In summary, photo-cross-linking induced both protein−protein interactions in the absence and presence of DNA and protein−DNA interactions in the presence of DNA.

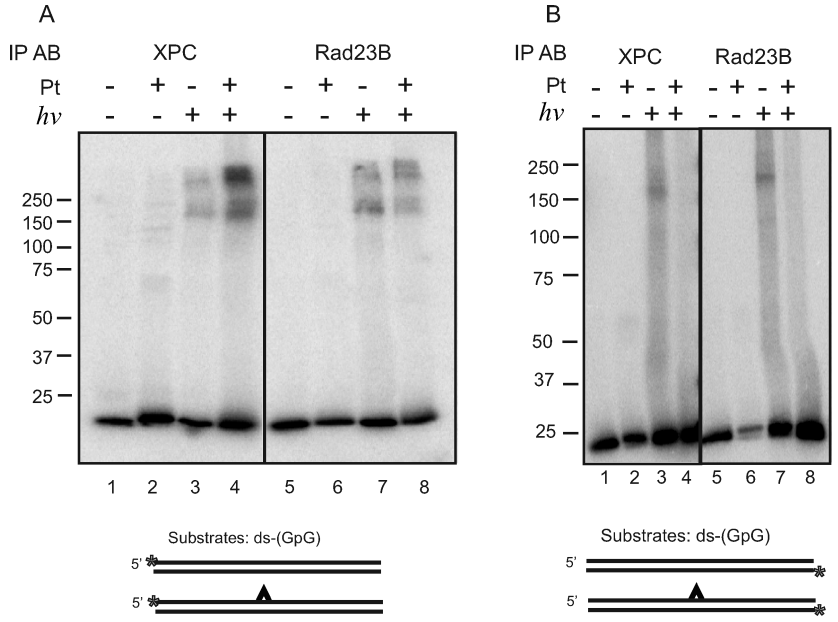

FIGURE 4: Immunoprecipitation of the photo-cross-linked protein−DNA complex with anti-XPC or anti-Rad23B. (A) XPC−Rad23B was bound and photo-cross-linked to radiolabeled undamaged or cisplatin-damaged double-stranded substrates containing the ^{32}P label on the damaged strand. IP was performed with either the XPC (lanes 1−4) or Rad23B antibody (lanes 5−8), and products were imaged using a PhosphorImager. (B) Reactions were performed in a manner similar to those in panel A except the ^{32}P label was on the DNA strand complementary to the damaged strand. A schematic of DNA substrates below each gel is presented with the cisplatin indicated by the carat and the position of the ^{32}P label by the asterisk.

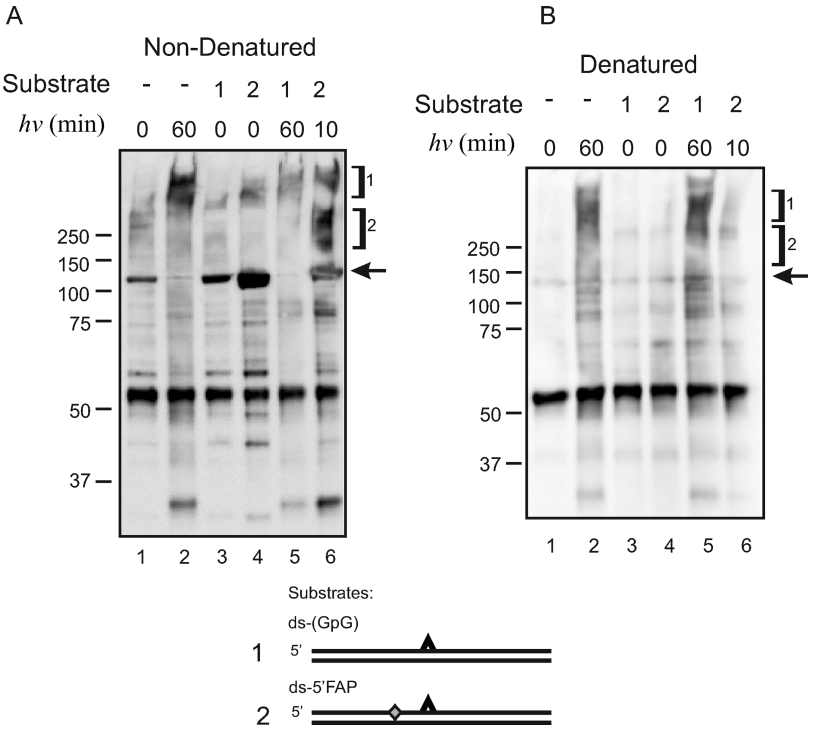

FIGURE 5: Immunoprecipitation and Western blot analysis of photo-cross-linked XPC in the absence or presence of damaged DNA. (A) XPC−Rad23B and the indicated DNA substrates were bound, cross-linked for the indicated time, and immunoprecipitated using the anti-Rad23B antibody. The immunoprecipitate was then separated via SDS−PAGE, transferred to PVDF, and probed with the anti-XPC antibody. Antibody reactivity was visualized by chemiluminescence detection using a HRP-conjugated secondary antibody. Bracket 1 denotes a covalent protein−protein cross-link that occurs between XPC and Rad23B subunits that is independent of DNA. Bracket 2 indicates a covalent protein−DNA cross-link. Free, un-cross-linked XPC is indicated by the arrow. (B) Identical reactions were performed as described for panel A except the samples were heat denatured prior to immunoprecipitation.

Together, these results lead to a model in which the XPC subunit is responsible for the majority of the interactions with DNA while Rad23B appears to make minimal contact directly with DNA (Figure 6). XPC−Rad23B does contact DNA to the 5′ and 3′ sides of the damaged site, though there appears to be a preference for interaction to the 5′ side of the lesion. XPC−Rad23B also makes contact with the undamaged strand, and in this case, the Rad23B subunit contributes to the interaction with

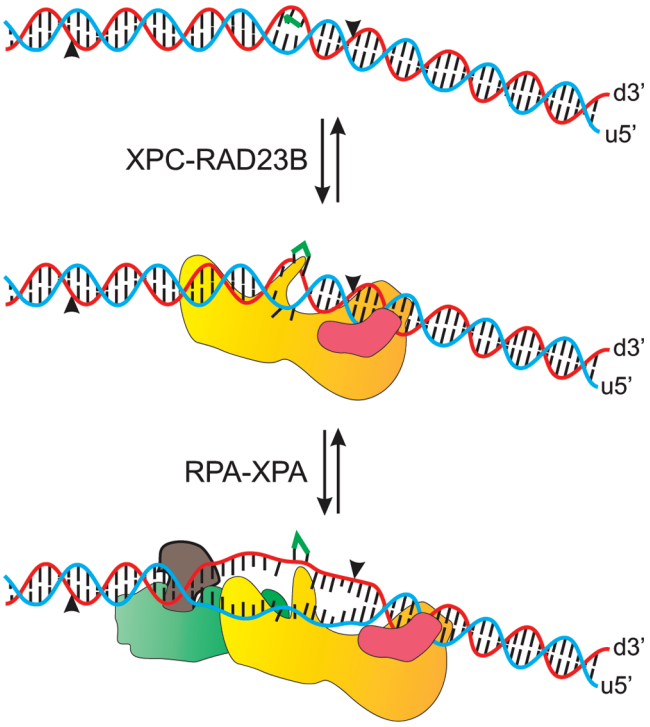

FIGURE 6: Model for binding of XPC−Rad23B to cisplatin-damaged DNA. XPC is presented as a yellow complex, Rad23B as a mauve complex, XPA as a brown complex, and RPA as a green complex. XPC−Rad23B recognizes and binds to cisplatin-damaged DNA with placement of the XPC subunit to the 5′ and 3′ sides of the cisplatin lesion. The Rad23B subunit interacts with the undamaged strand of the cisplatin-damaged duplex to the 3′ side of the cisplatin lesion. After damage recognition, RPA−XPA binds to the damaged duplex and XPC−Rad23B prepares to dissociate from the damaged DNA duplex.

DNA (Figure 6). Interestingly, the photo-cross-linking procedure resulted in the formation of a covalent bond between the two protein subunits that was not influenced by DNA, suggesting that the interface between these two protein subunits, following DNA binding, is not (or minimally) disrupted.

DISCUSSION

XPC−Rad23B as a DNA binding protein recognizes and interacts with the bases or the sugar−phosphate backbone of DNA. To impart damage specificity in the NER pathway, XPC−Rad23B must display a higher affinity for DNA containing chemical modifications or distortions. These can be caused by exposure to common chemotherapeutic agents like cisplatin or environmental carcinogens such as exposure to UV light. After binding to damaged DNA, XPC−Rad23B recruits downstream NER proteins and then dissociates from the site of damage prior to being incised by the XPG and XPF/ERCC1 nucleases (*1*, *2*). The binding and dissociation of XPC−Rad23B occur without any change in the chemical structure of the DNA, although changes in DNA secondary structure are likely to accompany XPC−Rad23B−DNA interactions (*21*). On the basis of the crystal structure analysis of the Rad4−Rad23B complex bound to UV-damaged DNA, changes in the secondary structure of DNA include the displacement of bases opposite the thymine dimer out of the DNA helix, and this is accompanied by localized unwinding of the DNA surrounding the lesion, possibly influencing DNA−protein interactions. Similarly, there are changes in the Rad4 protein tertiary structure in which the β-hairpins of BHD2 and BHD3 are inserted between the UV-damaged duplex DNA while in the apo structure these domains are displaced to avoid steric interaction (*21*). The cross-linking analysis performed in this study using cisplatin-damaged DNA revealed XPC−DNA interactions in the proximity of the cisplatin lesion, suggesting that while UV and cisplatin cause different DNA structural and chemical distortions, there is a common mechanism of damage recognition involving BHD2 and BHD3. More specifically, BHD3, which shares 31% sequence identity with XPC, may play a major role in stabilizing XPC−DNA interactions since most of the conserved regions are localized in residues with structural or DNA binding properties. The ability to photo-cross-link XPC−Rad23B to undamaged DNA is likely through the TGD and BHD1 domains as revealed from the crystal structure modeled with undamaged DNA (*21*). This suggests that the interaction of XPC−Rad23B with cisplatin-damaged DNA would be similar to that of the Rad4−Rad23B complex with UV-damaged DNA.

With respect to damage and DNA strand orientation, the majority of DNA interactions in the Rad4 structure are to the 3′ side of the DNA damage (*21*). Interestingly, the cross-linking analysis of XPC−Rad23B demonstrates interactions on both the 5′ and 3′ sides of the cisplatin lesion. The potential exists that photoinduced cross-linking of XPC−Rad23B to photoreactive DNA substrates may be influenced by the presence of the photoreactive FAP-dCMP analogue. However, cross-linking analysis, in which the analogue was incorporated into the complementary strand, either to the 5′ or to the 3′ side of the cisplatin adduct, demonstrates no difference in cross-linking of XPC−Rad23B to the DNA substrates (Figure 4 of the Supporting Information). The complete C-terminal and N-terminal domains of the Rad4 protein are absent in the crystal structure; however, the directionality of the protein domain location is suggestive of an interaction to the 5′ side of the lesion. However, further structural analysis is necessary to have a full assessment of the protein−DNA interaction. The cross-linking analysis reveals that XPC interacts with both the damaged and undamaged strands of the DNA duplex. The absence of structural data with the C-terminus of Rad4 makes the identification of amino acids interacting to the 5′ side of the damaged site impossible. However, structural analysis suggests that interactions of Rad4 with DNA to the 3′ side of the CPD lesion involve amino acids Val_{448}−Thr_{456}. Interactions of Rad4 with the undamaged strand of the duplex DNA are likely to occur via amino acids Lys_{511}−Leu_{531}. The interactions identified by the Rad4 crystal structure were based on DNA containing a CPD lesion; however, it is suggestive that the amino acids in contact with the DNA surrounding an adduct would be the same. In the case of the CPD lesion presented, amino acids Phe_{599}−Val_{605} insert between the two DNA strands of the duplex and interact with nucleotides directly surrounding the CPD adduct (*21*). As a cisplatin intrastrand lesion distorts the DNA differently than a CPD lesion, the interaction of XPC−Rad23B with the damaged DNA may in fact be different, with the difference in distortion resulting in the differential positioning of XPC on the damaged duplex. This would then potentially influence the binding and placement of downstream NER proteins and impact the position of incision relative to the adduct. While previously published data have demonstrated that the size of the incised fragment is the same with platinum and UV adducts (*35*), the position of XPG- and XPF-catalyzed incision on cisplatin-damaged DNA is not known.

While initial cross-linking and immunoprecipitation experiments with XPC−Rad23B were suggestive of a direct Rad23B−DNA covalent cross-link, further analysis demonstrates that Rad23B does not interact directly with DNA; the interaction occurs through the XPC subunit. Cross-linking analysis alone does not demonstrate the presence of a Rad23B−DNA interaction because if a covalent interaction was induced by photo-cross-linking, a complex between 60 and 100 kDa would be present. Therefore, one must be cautious in the interpretation of data with multisubunit proteins assessing DNA−protein interactions due to the possibility of protein−protein cross-links. This also highlights the tremendous utility for the use of photoreactive analogues with high photometric yields for the identification of true protein−DNA covalent cross-links without the induction of UV-induced protein−protein cross-links. On the basis of the data presented and previous structural data involving Rad4 (*21*), the model depicts that XPC−Rad23B interacts with both strands of a cisplatin-damaged duplex DNA. The XPC subunit interacts both to the 5′ and to the 3′ side of the cisplatin adduct and contacts both the damaged strand and the undamaged strand of the duplex. The Rad23B subunit also interacts with both strands of the duplex DNA and contacts the XPC subunit directly. Following damage recognition and binding of XPC−Rad23B, the duplex DNA opens, allowing the RPA−XPA complex to bind to the damaged DNA (*2*). The model depicts an RPA−XPA interaction to the 5′ side of the cisplatin lesion contacting the undamaged DNA strand. The structure of the DNA is further altered by the addition of the RPA−XPA complex and continues to generate a larger single-stranded region with the addition of downstream NER proteins, such as TFIIH, XPF, and XPG.

In vitro, the XPC−Rad23B heterodimer is sufficient to reconstitute the NER damage recognition complex and supports dual incision (*36*). In vivo, Centrin 2 forms a complex with XPC−Rad23B, and how Centrin 2 influences these protein−DNA interactions in the cell remains unknown. Similarly, XPC is subject to extensive post-translation modifications such as ubiquitination and sumolyation which can impact DNA binding and protein−protein interactions (*37*, *38*). It has been shown that XPC is reversibly ubiquitinated by DDB; however, this ubiquitination does not trigger XPC degradation (*37*), and it remains unknown how, after damage recognition, XPC−Rad23B is released from the site of damage. It is possible that post-translational modifications may influence the XPC−Rad23B−DNA interaction and cause XPC−Rad23B to dissociate from the damaged site. Taken together, it will also be of interest to determine the role of Centrin 2, DDB, and post-translational modifications in XPC−Rad23B−DNA interactions to provide better insight into the mechanisms of damage recognition and dissociation of XPC−Rad23B from damaged DNA.

ACKNOWLEDGMENT

We thank the members of the Turchi lab for their insightful scientific discussions and detailed reading of the manuscript.

SUPPORTING INFORMATION AVAILABLE

Flowchart for substrate preparation, photo-cross-linking analysis involving a 1,3-cisplatin lesion, and photo-cross-linking analysis in which the photoreactive analogue is located to the 3′ side of the cisplatin lesion or in the complementary strand. This material is available free of charge via the Internet at http://pubs.acs.org.

REFERENCES

1. Nouspikel, T. (2009) DNA repair in mammalian cells: Nucleotide excision repair: Variations on versatility. *Cell. Mol. Life Sci. 66*, 994–1009.
2. Shuck, S. C., Short, E. A., and Turchi, J. J. (2008) Eukaryotic nucleotide excision repair: From understanding mechanisms to influencing biology. *Cell Res. 18*, 64–72.
3. Sugasawa, K., Ng, J. M. Y., Masutani, C., Iwai, S., vanderSpek, P. J., Eker, A. P. M., Hanaoka, F., Bootsma, D., and Hoeijmakers, J. H. J. (1998) Xeroderma pigmentosum group C protein complex is the initiator of global genome nucleotide excision repair. *Mol. Cell 2*, 223–232.
4. Wakasugi, M., and Sancar, A. (1999) Order of assembly of human DNA repair excision nuclease. *J. Biol. Chem. 274*, 18759–18768.
5. Araujo, S. J., Tirode, F., Coin, F., Pospiech, H., Syvaoja, J. E., Stucki, M., Hubscher, U., Egly, J. M., and Wood, R. D. (2000) Nucleotide excision repair of DNA with recombinant human proteins: Definition of the minimal set of factors, active forms of TFIIH, and modulation by CAK. *Genes Dev. 14*, 349–359.
6. Lehmann, A. R. (2006) New functions for Y family polymerases. *Mol. Cell 24*, 493–495.
7. Tapias, A., Auriol, J., Forget, D., Enzlin, J. H., Scharer, O. D., Coin, F., Coulombe, B., and Egly, J. M. (2004) Ordered conformational changes in damaged DNA induced by nucleotide excision repair factors. *J. Biol. Chem. 279*, 19074–19083.
8. Nishi, R., Alekseev, S., Dinant, C., Hoogstraten, D., Houtsmuller, A. B., Hoeijmakers, J. H., Vermeulen, W., Hanaoka, F., and Sugasawa, K. (2009) UV-DDB-dependent regulation of nucleotide excision repair kinetics in living cells. *DNA Repair 8*, 767–776.
9. Sugasawa, K. (2009) UV-DDB: A molecular machine linking DNA repair with ubiquitination. *DNA Repair 8*, 969–972.
10. Wakasugi, M., Kawashima, A., Morioka, H., Linn, S., Sancar, A., Mori, T., Nikaido, O., and Matsunaga, T. (2002) DDB Accumulates at DNA Damage Sites Immediately after UV Irradiation and Directly Stimulates Nucleotide Excision Repair. *J. Biol. Chem. 277*, 1637–1640.
11. El-Mahdy, M. A., Zhu, Q., Wang, Q. E., Wani, G., Praetorius-Ibba, M., and Wani, A. A. (2006) Cullin 4A-mediated proteolysis of DDB2 protein at DNA damage sites regulates in vivo lesion recognition by XPC. *J. Biol. Chem. 281*, 13404–13411.
12. Araki, M., Masutani, C., Takemura, M., Uchida, A., Sugasawa, K., Kondoh, J., Ohkuma, Y., and Hanaoka, F. (2001) Centrosome protein centrin 2/caltractin 1 is part of the xeroderma pigmentosum group C complex that initiates global genome nucleotide excision repair. *J. Biol. Chem. 276*, 18665–18672.
13. Aboussekhra, A., Biggerstaff, M., Shivji, M. K., Vilpo, J. A., Moncollin, V., Podust, V. N., Protic, M., Hubscher, U., Egly, J. M., and Wood, R. D. (1995) Mammalian DNA nucleotide excision repair reconstituted with purified protein components. *Cell 80*, 859–868.
14. Park, C. H., and Sancar, A. (1993) Reconstitution of mammalian excision repair activity with mutant cell-free extracts and XPAC and ERCC1 proteins expressed in *Escherichia coli*. *Nucleic Acids Res. 21*, 5110–5116.
15. Krasikova, Y. S., Rechkunova, N. I., Maltseva, E. A., Petruseva, I. O., Silnikov, V. N., Zatsepin, T. S., Oretskaya, T. S., Scharer, O. D., and Lavrik, O. I. (2008) Interaction of nucleotide excision repair factors XPC-HR23B, XPA, and RPA with damaged DNA. *Biochemistry* (*Moscow, Russ. Fed.*) *73*, 886–896.
16. Trego, K. S., and Turchi, J. J. (2006) Pre-steady state binding of damaged DNA by XPC-hHR23B reveals a kinetic mechanism for damage discrimination. *Biochemistry 45*, 1961–1969.
17. Sugasawa, K., Okamoto, T., Shimizu, Y., Masutani, C., Iwai, S., and Hanaoka, F. (2001) A multistep damage recognition mechanism for global genomic nucleotide excision repair. *Genes Dev. 15*, 507–521.
18. You, J. S., Wang, M., and Lee, S. H. (2003) Biochemical analysis of the damage recognition process in nucleotide excision repair. *J. Biol. Chem. 278*, 7476–7485.
19. Roche, Y., Zhang, D., Segers-Nolten, G. M., Vermeulen, W., Wyman, C., Sugasawa, K., Hoeijmakers, J., and Otto, C. (2008) Fluorescence correlation spectroscopy of the binding of nucleotide excision repair protein XPC-hHr23B with DNA substrates. *J. Fluoresc. 18*, 987–995.
20. Maillard, O., Solyom, S., and Naegeli, H. (2007) An aromatic sensor with aversion to damaged strands confers versatility to DNA repair. *PLoS Biol. 5*, e79.

21. Min, J. H., and Pavletich, N. P. (2007) Recognition of DNA damage by the Rad4 nucleotide excision repair protein. *Nature 449*, 570–575.
22. Rigas, J. R., and Kelly, K. (2007) Current treatment paradigms for locally advanced non-small cell lung cancer. *J. Thorac. Oncol. 2* (Suppl. 2), S77–S85.
23. Juergens, R. A., and Brahmer, J. R. (2005) Adjuvant therapy for resected non-small-cell lung cancer: Past, present, and future. *Curr. Oncol. Rep. 7*, 248–254.
24. Einhorn, L. H. (2002) Curing metastatic testicular cancer. *Proc. Natl. Acad. Sci. U.S.A. 99*, 4592–4595.
25. Armstrong, D. K., Bundy, B., Wenzel, L., Huang, H. Q., Baergen, R., Lele, S., Copeland, L. J., Walker, J. L., and Burger, R. A. (2006) Intraperitoneal cisplatin and paclitaxel in ovarian cancer. *N. Engl. J. Med. 354*, 34–43.
26. Teuben, J. M., Bauer, C., Wang, A. H. J., and Reedijk, J. (1999) Solution structure of a DNA duplex containing a cis-diammineplatinum(II) 1,3-d(GTG) intrastrand cross-link, a major adduct in cells treated with the anticancer drug carboplatin. *Biochemistry 38*, 12305–12312.
27. Liedert, B., Pluim, D., Schellens, J., and Thomale, J. (2006) Adduct-specific monoclonal antibodies for the measurement of cisplatin-induced DNA lesions in individual cell nuclei. *Nucleic Acids Res. 34*, e47.
28. Dezhurov, S. V., Khodyreva, S. N., Plekhanova, E. S., and Lavrik, O. I. (2005) A new highly efficient photoreactive analogue of dCTP. Synthesis, characterization, and application in photoaffinity modification of DNA binding proteins. *Bioconjugate Chem. 16*, 215–222.
29. Manley, J. L., Fire, A., Cano, A., Sharp, P., and Gefter, M. L. (1980) DNA-dependent transcription of adenovirus genes is a soluble whole cell extract. *Proc. Natl. Acad. Sci. U.S.A. 77*, 3855–3859.
30. Park, C. J., and Choi, B. S. (2006) The protein shuffle. Sequential interactions among components of the human nucleotide excision repair pathway. *FEBS J. 273*, 1600–1608.
31. Lippard, S. J., Bond, P. J., WU, K. C., and Bauer, W. R. (1976) Stereochemical requirements for intercalation of platinum complexes into double-stranded DNA's. *Science 194*, 726–728.
32. Hermanson-Miller, I. L., and Turchi, J. J. (2002) Strand-specific binding of RPA and XPA to damaged duplex DNA. *Biochemistry 41*, 2402–2408.
33. Maltseva, E. A., Rechkunova, N. I., Gillet, L. C., Petruseva, I. O., Scharer, O. D., and Lavrik, O. I. (2007) Crosslinking of the NER damage recognition proteins XPC-HR23B, XPA and RPA to photoreactive probes that mimic DNA damages. *Biochim. Biophys. Acta 1770*, 781–789.
34. Khodyreva, S. N., and Lavrik, O. I. (2005) Photoaffinity labeling technique for studying DNA replication and DNA repair. *Curr. Med. Chem. 12*, 641–655.
35. Zamble, D. B., Mu, D., Reardon, J. T., Sancar, A., and Lippard, S. J. (1996) Repair of cisplatin−DNA adducts by the mammalian excision nuclease. *Biochemistry 35*, 10004–10013.
36. Mu, D., Park, C. H., Matsunaga, T., Hsu, D. S., Reardon, J. T., and Sancar, A. (1995) Reconstitution of human DNA repair excision nuclease in a highly defined system. *J. Biol. Chem. 270*, 2415–2418.
37. Sugasawa, K., Okuda, Y., Saijo, M., Nishi, R., Matsuda, N., Chu, G., Mori, T., Iwai, S., Tanaka, K., Tanaka, K., and Hanaoka, F. (2005) UV-induced ubiquitylation of XPC protein mediated by UV-DDB-ubiquitin ligase complex. *Cell 121*, 387–400.
38. Wang, Q. E., Zhu, Q. Z., Wani, G., El-Mahdy, M. A., Li, J. Y., and Wani, A. A. (2005) DNA repair factor XPC is modified by SUMO-1 and ubiquitin following UV irradiation. *Nucleic Acids Res. 33*, 4023–4034.